Inorg. Chem. **1983**, *22*, 3645-3653

Contribution from the Departments of Chemistry, Drexel University, Philadelphia, Pennsylvania 19104,
The Polytechnic of North London, London N7 8DB, England, and the University of Virginia, Charlottesville, Virginia 22901

Pentacoordinate Copper Complexes of Nitrogen–Sulfur Donors: Structural Chemistry of Two Complexes of Bis(2-(2-benzimidazolyl)ethyl) Sulfide with the Sulfur Alternatively in Equatorial and Axial Coordination Modes

ANTHONY W. ADDISON,*[1a] PHILIP J. BURKE,[1a] KIM HENRICK,[1b] T. NAGESWARA RAO,[1a] and EKKEHARD SINN[1c]

Received March 24, 1983

Simple and mixed-ligand copper(II) complexes were synthesized and characterized by crystallographic and spectroscopic techniques. The N,S- and O-donor chelating agents used include the following: 1,5-bis(benzimidazol-2-yl)-3-thiapentane, BBES; 1,5-bis(*N*-methylbenzimidazol-2-yl)-3-oxopentane, Me_2BBEO; 2,5,8-trimethyl-2,5,8-triazanonane, pmeta; pentane-2,4-dionate anion, $acac^-$; 2,2′-bipyridyl, bpy; 2,2′-biimidazole, biim. The perchlorate of Cu(BBES) crystallizes from methanol as the salt $[Cu(BBES)(MeOH)(OH_2)](ClO_4)_2$, with the symmetry of the space group $P\bar{1}$, $Z = 2$, $a = 9.306$ (3) Å, $b = 10.072$ (5) Å, $c = 14.194$ (5) Å, $\alpha = 92.23$ (2)°, $\beta = 96.63$ (4)°, $\gamma = 108.56$ (3)°, and $\rho_{calcd} = 1.66$ g·cm^{-3}. The structure was solved with the Patterson method, incorporating 3088 of the 3884 independent reflections, to final *R* values of 5.6% and 6.1% (R_w). The complex cation has a distorted tetragonal pentacoordinate structure ($\tau = 0.27$) with the BBES occupying three equatorial positions, with a Cu–S linkage of 2.297 Å, and the methanol bound axially. This contrasts with the perchlorate salt of a similar ligand's complex, obtained from ethanol, which has a perchlorate coordinated at this axial position. $[Cu(BBES)(acac)]PF_6{\cdot}H_2O{\cdot}EtOH$ was recrystallized from ethyl acetate to give the ester solvate, $[Cu(BBES)(acac)]PF_6{\cdot}C_4H_8O_2$. This complex also crystallizes with symmetry $P\bar{1}$, and $Z = 2$, $a = 13.961$ (3) Å, $b = 12.892$ (3) Å, $c = 10.154$ (3) Å, $\alpha = 101.57$ (4)°, $\beta = 104.99$ (4)°, $\gamma = 104.34$ (4)°, and $\rho_{calcd} = 1.160$ g·cm^{-3}. The structure was solved by the Patterson method, using 2939 of the 3243 independent reflections, to final *R* values of 6.3% and 6.1% (R_w). The complex cation is of regularly tetragonal pyramidal geometry ($\tau = 0.02$) with an equatorial N_2O_2-donor set and the thioether bound axially at 2.696 Å, in contrast to the Cu(BBES) perchlorates. There are hydrogen-bonding interactions with benzimidazole and water protons in the lattices of the complexes. ESR spectroscopy shows that the $Cu(BBES)^{2+}$ and $Cu(Me_2BBEO)^{2+}$ complexes retain their distorted structures in solution; both give single-line ESR spectra in solution at ambient temperatures. The $[Cu(BBES)(acac)]^+$ salts exhibit pairwise dipolar coupling in their crystalline states. Substitution of ether by thioether as donor causes absorptivity enhancement throughout the visible–near-UV spectrum, and difference spectroscopy has been used to assign sulfur-to-copper charge-transfer transitions. Unlike $[Cu(bpy)(acac)]^+$ and $[Cu(BBES)(acac)]^+$, the complex cations $[Cu(Me_2BBEO)(acac)]^+$ and $[Cu(biim)(acac)]^+$ are unstable toward coordinative disproportionation in the solvents used. The $Cu(BBES)^{2+}$ cation in solution is in equilibrium between the *fac*-BBES and *mer*-BBES isomers, the latter being dominant.

Introduction

Confirmation of the coordination of methionyl sulfur in the copper proteins *Populus nigra* var. italica plastocyanin[2] and *Pseudomonas aeruginosa* azurin[3] has greatly stimulated the systematic investigation of thioether complexes of copper(I) and copper(II). The simultaneous occurrence of histidyl imidazole in these irregularly shaped coordination spheres has led to a flurry of N(heterocyclic)–S(thioether) ligand development,[4-7] and the oligodentate benzimidazole systems introduced recently by Thompson and co-workers[8] have, in particular, led to a new class of imidazolyl–thioether ligands.[9]

In continuing our interest[10] in the relationships between natural and synthetic systems, we have recently described[11] a copper(II)–mercaptide system with axial Cu–S linkages similar to the axial Cu–S(Met) bond in plastocyanin and a distorted pentacoordinate complex entailing benzimidazole–thioether N_2S_2 coordination.[12] We report herein on properties of two pentacoordinate complexes of a thioether–benzimidazole ligand, BBES (Figure 1), in which the $CuSN_2O_2$ cores are isomeric, with respect to the arrangement of the S, O, and N donor atoms. One of the complexes also contains the anion of pentane-2,4-dione (acacH) as a ligand.

During the course of this work, the synthesis and structure were published[7] of a copper(II) complex of a very similar ligand, TMBBES. This is a derivative of BBES with the benzimidazole rings methylated at the 5-, 5′-, 6-, and 6′-positions. However, it transpires that our Cu(BBES) perchlorate has a different copper coordination environment in the solid state.

Experimental Section

Reagents were used as received from Aldrich, Sigma (organics), G. F. Smith, and Fluka (copper perchlorate). Mass spectra and NMR spectra were recorded on Finnigan 4000 GC–MS and JEOL FX90Q instruments, Me_4Si being used as internal standard in the latter. Optical spectra were obtained from Cary 14 and Perkin-Elmer 320 spectrophotometers and ESR spectra on a Varian E-12 X-band instrument, calibrated with DPPH and $VO(acac)_2$ near $g = 2$. The values of g_0 and A_0 were measured at ambient temperature, and $g_\parallel$, $A_\parallel$, and $g_\perp$ (approximated by the center of the N shf) were measured at 77 K. $A_\perp$ was computed as $^1/_2(3A_0 - A_\parallel)$. Second-order corrections[13] were applied to the resonance fields of the transitions from which g_0 and A_0 were obtained.

Syntheses. BBES was synthesized by published procedures.[9,14]

---

[1] (a) Drexel University. (b) The Polytechnic of North London. (c) University of Virginia.

[2] Colman, P. M.; Freeman, H. C.; Guss, J. M.; Murata, M.; Norris, V. A.; Ramshaw, J. A. M.; Venkatappa, M. P. *Nature (London)* **1978**, *272*, 319.

[3] Adman, E. T.; Stenkamp, R. E.; Sieker, L. C.; Jensen, L. H. *J. Mol. Biol.* **1978**, *123*, 35.

[4] Thompson, J. S.; Zitzmann, J. L.; Marks, T. J.; Ibers, J. A. *Inorg. Chim. Acta* **1980**, *46*, L101.

[5] Brubaker, G. R.; Brown, J. N.; Yoo, M. K.; Kinsey, R. A.; Kutchan, T. M.; Mottel, E. A. *Inorg. Chem.* **1979**, *18*, 299.

[6] Rietmeyer, F. J.; Birker, P. J. M. W. L.; Gorter, S.; Reedijk, J. *J. Chem. Soc., Dalton Trans.* **1982**, 1191.

[7] Dagdigian, J. V.; McKee, V.; Reed, C. A. *Inorg. Chem.* **1982**, *21*, 1332.

[8] Thompson, L. K.; Ramaswamy, B. S.; Seymour, E. A. *Can. J. Chem.* **1977**, *55*, 878.

[9] Dagdigian, J. V.; Reed, C. A. *Inorg. Chem.* **1979**, *18*, 2623.

[10] Sakaguchi, U.; Addison, A. W. *J. Chem. Soc., Dalton Trans.* **1979**, 600.

[11] Addison, A. W.; Sinn, E. *Inorg. Chem.* **1983**, *22*, 1225.

[12] Addison, A. W.; Rao, T. N.; Reedijk, J.; van Rijn, J.; Verschoor, G., submitted for publication.

[13] (a) Ingram, D. J. E. "Spectroscopy at Radio and Microwave Frequencies"; Butterworths: London, 1955; p 305. (b) Kosman, D.; Bereman, R. In "Spectroscopy in Biochemistry"; Bell, J. E., Ed.; CRC Press: Boca Raton, FL, 1981; Vol. II, Chapter 2. The expression for the second-order correction to the resonance fields for $g_\parallel$ should contain $A_\perp$ rather than $A_\parallel$.

0020-1669/83/1322-3645$01.50/0

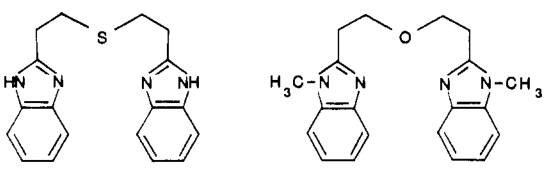

Figure 1. The ligands BBES (left) and Me_2BBEO (right).

1,5-Bis(*N*-methylbenzimidazol-2-yl)-3-oxopentane, Me_2BBEO. A 1.24-g (10 mmol) amount of bis(2-cyanoethyl) ether (Frinton Laboratories) was refluxed with 3.9 g (20 mmol) of *N*-methyl-*o*-phenylenediamine in 150 mL of 4 M HCl for 17 h. The reaction mixture was cooled to room temperature and treated with an excess of 5 M NaOH. The pink solid that separated was filtered off, washed with cold water, and recrystallized from 25 mL of THF (charcoal) by addition of excess ice-cold *n*-hexane. The white crystalline product was filtered off and dried in vacuo over potassium hydroxide; mp 116 °C (uncor). Anal. Calcd for $C_{20}H_{22}N_4O{\cdot}H_2O$: C, 68.2; H, 6.81; N, 15.9. Found: C, 68.9; H, 6.86; N, 16.4. MS: 334 (8%, M^+) and more intense peaks at 175 (20%), 159 (100%), 146 (70%), 131 (30%), 77 (40%), 51 (20%). NMR (δ values in deuteriochloroform) 3.03 ($-CH_2-$, t, J = 6.6 Hz), 3.45 ($-CH_3$, s), 3.93 ($-O-CH_2-$, t, J = 6.6 Hz), 7.14 (Bzim-5,6, m), 7.17 (Bzim-4,7, m).

Copper(II) Complex of BBES: $Cu(BBES)(ClO_4)_2{\cdot}H_2O{\cdot}CH_3OH$. 1,5-Bis(2-benzimidazolyl)-3-thiapentane (1.61 g, 5 mmol) was dissolved in 50 mL of methanol and added to $Cu(ClO_4)_2{\cdot}6H_2O$ (1.85 g, 5 mmol) also in 50 mL of methanol. The resulting dark green solution was evaporated at room temperature to a small volume (15 mL) to give dark green crystals of the complex. The crystals were filtered off and air-dried. Anal. Calcd for $C_{19}H_{24}Cl_2CuN_4O_{10}S$: C, 35.9; H, 3.78; N, 8.82. Found: C, 35.4; H, 3.60; N, 8.67.

Copper(II) Complex of Me_2BBEO: $[Cu(Me_2BBEO)_2](ClO_4)_2{\cdot}H_2O$. A 0.37-g (1 mmol) amount of $Cu(ClO_4)_2{\cdot}6H_2O$ dissolved in 15 mL of methanol was added to 0.33 g (1 mmol) of Me_2BBEO also in 15 mL of methanol. The mixture was refluxed for 20 min and then filtered. Slow evaporation of the solvent gave blue prisms, which were filtered off, washed with the minimum amount of water, and air-dried. Anal. Calcd for $CuC_{40}H_{46}N_8O_{11}Cl_2$: C, 50.6; H, 4.84; N, 11.8. Found: C, 50.4; H, 4.97; N, 11.9. The 1:2 complex is obtained, despite the 1:1 reactant ratio. The same product was also obtained when the synthesis of $[Cu(Me_2BBEO)(acac)]ClO_4$ was attempted.

(Pentane-2,4-dionato)(1,5-bis(benzimidazol-2-yl)-3-thiapentane)-copper(II) Hexafluorophosphate–water–ethanol (1/1/1), $[Cu(BBES)(acac)]PF_6{\cdot}H_2O{\cdot}C_2H_5OH$, was prepared by refluxing copper(II) perchlorate hexahydrate (1.15 g, 3.1 mmol), BBES (1.0 g, 3.1 mmol), Et_3N (0.31 g, 3.1 mmol), and acacH (0.31 g, 3.1 mmol) in methanol solution (100 mL) for 30 min. Addition of saturated aqueous KPF_6 solution (100 mL) to the hot reaction mixture gave a blue-green precipitate, which was collected by filtration and recrystallized from an ethanol–water mixture to give the complex. Anal. Calcd for $C_{25}H_{27}N_4O_2SCuPF_6{\cdot}H_2O{\cdot}C_2H_5OH$: C, 43.3; H, 4.79; N, 8.07. Found: C, 42.8; H, 4.37; N, 7.89. The pale blue platelets obtained proved unsuitable for X-ray diffraction. Recrystallization from ethyl acetate yielded crystals of more suitable habit. The H_2O–ethanol solvate is referred to hereafter as the hydrate.

(2,2′-Bipyridyl)(pentane-2,4-dionato)copper(II) perchlorate–methanol (1/1), $[Cu(bpy)(acac)](ClO_4){\cdot}CH_3OH$, was prepared by addition of a solution of pentane-2,4-dione (3 mmol) and triethylamine (3 mmol) in warm methanol (10 mL) to hydrated copper(II) perchlorate (3 mmol) in warm methanol (10 mL), followed by 2,2′-bipyridyl (3 mmol) in methanol (10 mL). After brief refluxing, the product crystallized as the solution cooled, and grey-blue prisms in 80% yield were collected by filtration, washed with cold methanol, and dried in vacuo over P_4O_{10}. Anal. Calcd for $C_{15}H_{15}CuN_2O_2{\cdot}ClO_4{\cdot}CH_3OH$: C, 42.7; H, 4.25; N, 6.22. Found: C, 43.0; H, 4.32; N, 6.26.

(2,5,8-Trimethyl-2,5,8-triazanonane)(pentane-2,4-dionato)copper(II) perchlorate, $[Cu(pmeta)(acac)]ClO_4$, was prepared by a procedure similar to that above, with 5 mmol each of pentane-2,4-dione, copper(II) perchlorate, sodium hydroxide, and the triamine (1,1,4,7,7-pentamethyldiethylenetriamine, Ames Laboratories). After addition of water, filtration, and (rotary) evaporation, deep greenish blue crystals were obtained. These were filtered off, washed with water, and air-dried (efflorescence). Anal. Calcd for $C_{14}H_{30}CuN_3O_2{\cdot}ClO_4$: C, 38.6; H, 6.95; N, 9.65. Found: C, 39.0; H, 7.06; N, 9.57.

Table I. Crystal Data for $[Cu(BBES)(CH_3OH)(OH_2)](ClO_4)_2$

space group $P\bar{1}$ (triclinic)	$\alpha = 92.23\ (2)°$
$Z = 2$	$\beta = 96.63\ (4)°$
$a = 9.306\ (3)$ Å	$\gamma = 108.56\ (3)°$
$b = 10.072\ (5)$ Å	$V = 1248$ Å^3
$c = 14.194\ (5)$ Å	$\rho_{calcd} = 1.66\ g{\cdot}cm^{-3}$
	$\mu(Mo\ K\alpha) = 12.65\ cm^{-1}$

cryst dimens (face) to centroid mm: (100) 0.46, ($\bar{1}$00) 0.46, (010) 0.08, (0$\bar{1}$0) 0.08, (001) 0.13, (00$\bar{1}$) 0.13
mol wt ($C_{18}H_{24}Cl_2CuN_4O_{10}S$): 622.9
max, min transmission coeffs: 0.86, 0.81

no. of indep reflcns: 3884
$R_F = 5.6\%$
$R_{Fw} = 6.1\%$

Table II. Crystal Data for $[Cu(BBES)(acac)](PF_6){\cdot}C_4H_8O_2$

space group $P\bar{1}$ (triclinic)	$V = 1640.6$ Å^3
$Z = 2$	$\rho_{calcd} = 1.160\ g{\cdot}cm^{-3}$
$a = 13.961\ (3)$ Å	$\mu(Mo\ K\alpha) = 8.00\ cm^{-1}$
$b = 12.892\ (3)$ Å	cryst dimens: 0.21 × 0.16 × 0.18 mm
$c = 10.154\ (3)$ Å	mol wt ($C_{23}H_{25}CuN_4O_2SPF_6{\cdot}C_4H_8O_2$): 573.2
$\alpha = 101.57\ (4)°$	no. of indep reflcns: 3243
$\beta = 104.99\ (4)°$	
$\gamma = 104.34\ (4)°$	

2,2′-Biimidazole (biim) was prepared as described previously.[10] Because the absorption bands of this ligand are shifted more to the UV than those of 2,2′-bipyridyl (see Results and Discussion), we attempted to synthesize $[Cu(biim)(acac)]ClO_4$ but were not successful.

Crystallographic Data Collection and Structure Analyses: $[Cu(BBES)(MeOH)(OH_2)](ClO_4)_2$. Cell dimensions and space group data were obtained by standard methods on an Enraf-Nonius four-circle CAD-4 diffractometer. The θ–2θ scan technique was used, as previously described,[15] to record the intensities for all nonequivalent reflections for which $1° < 2\theta < 53°$. Scan widths were calculated as $(A + B \tan \theta)°$, where A is estimated from the mosaicity of the crystal and B allows for the increase in peak width due to $K\alpha_1 - K\alpha_2$ splitting. The values of A and B were 0.6 and 0.35°, respectively.

The intensities of three standard reflections showed no greater fluctuations during the data collection than those expected from Poisson statistics. The raw intensity data were corrected for Lorentz–polarization effects and absorption. A total of 3088 independent intensities, with $F_o^2 > 3\sigma(F_o^2)$, where $\sigma(F_o^2)$ was estimated from counting statistics,[16] were used in the final refinement of the structural parameters.

A three-dimensional Patterson synthesis was used to determine the heavy-atom positions, which phased the data sufficiently well to permit location of the remaining non-hydrogen atoms from Fourier syntheses. Full-matrix least-squares refinement was carried out as previously described.[15] Anisotropic temperature factors were introduced for the non-hydrogen atoms. The phenyl hydrogen atoms were inserted in their calculated positions. Further Fourier difference functions now permitted location of the other hydrogen atoms, which were included in the refinement for four cycles of least squares and then held fixed.

The model converged to a featureless final Fourier difference map. A listing of the observed and calculated structure factors is available together with calculated thermal parameters and selected least-squares planes through groups of atoms as supplementary material. The principal programs used are as described previously.[15]

Final positional parameters for the atoms are given in Table III. Table V contains the most important bond lengths and nearest intermolecular contacts and Table VI the significant bond angles. The digits in parentheses in the tables are the estimated standard deviations in the least significant figures quoted and were derived from the inverse matrix in the course of least-squares refinement calculations.

$[Cu(BBES)(acac)](PF_6){\cdot}C_4H_8O_2$. Reflections were collected in the range $3° \leq \theta \leq 25°$, with use of a Philips PW1100 diffractometer with Mo Kα radiation with a graphite monochromator (T = 22 °C).

---

(14) Addison, A. W.; Burke, P. J. *J. Heterocycl. Chem.* **1981**, *18*, 803.

(15) Freyberg, D. P.; Mockler, G. M.; Sinn, E. *J. Chem. Soc., Dalton Trans.* **1976**, 447.

(16) Corfield, P. W. R.; Doedens, R.; Ibers, J. A. *Inorg. Chem.* **1967**, *6*, 197.

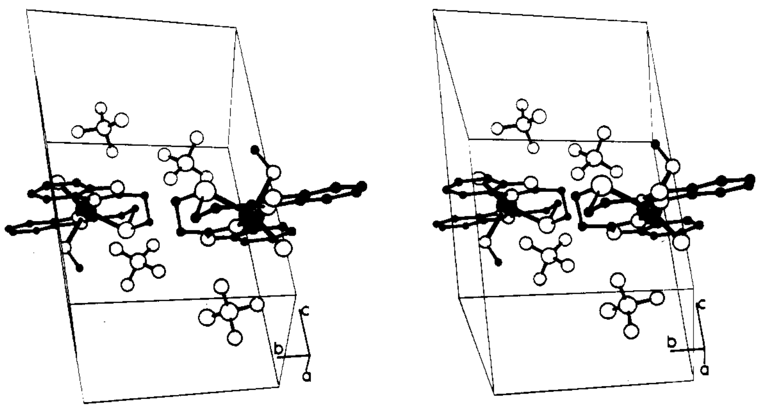

Figure 2. Unit cell of $[Cu(BBES)(MeOH)(OH_2)](ClO_4)_2$. Hydrogen atoms are omitted for clarity of presentation (ORTEP stereoview).

Table III. Fractional Atomic Coordinates for Non-Hydrogen Atoms of $[Cu(BBES)(MeOH)(OH_2)](ClO_4)_2$

atom	*x*	*y*	*z*
Cu	−0.11082 (9)	0.14867 (9)	0.23407 (6)
Cl(1)	0.2967 (2)	0.3554 (2)	0.6024 (1)
Cl(2)	0.1716 (2)	0.3035 (2)	0.0146 (1)
S	−0.1385 (2)	0.3462 (2)	0.3054 (1)
O(W)	−0.0713 (5)	0.0255 (6)	0.1336 (4)
O(Me)	−0.1835 (6)	0.0135 (6)	0.3550 (3)
O(1)	0.3605 (10)	0.2554 (9)	0.5786 (7)
O(2)	0.3873 (12)	0.4429 (12)	0.6752 (8)
O(3)	0.1680 (12)	0.2916 (16)	0.6403 (12)
O(4)	0.2911 (17)	0.4451 (12)	0.5394 (8)
O(5)	0.1684 (6)	0.1650 (6)	0.0338 (4)
O(6)	0.0525 (7)	0.3334 (7)	0.0574 (5)
O(7)	0.1399 (11)	0.3059 (10)	−0.0835 (5)
O(8)	0.3126 (9)	0.3950 (10)	0.0481 (10)
N(1a)	−0.3244 (6)	0.1067 (6)	0.1720 (4)
N(1b)	0.1083 (6)	0.1955 (6)	0.2842 (4)
N(3a)	−0.5446 (6)	0.1204 (7)	0.1067 (4)
N(3b)	0.3461 (7)	0.3130 (7)	0.3374 (5)
C(2a)	−0.4016 (7)	0.1927 (7)	0.1455 (5)
C(4a)	−0.5665 (7)	−0.0186 (8)	0.1083 (5)
C(5a)	−0.4261 (7)	−0.0280 (7)	0.1498 (4)
C(6a)	−0.4105 (8)	−0.1563 (8)	0.1628 (5)
C(7a)	−0.5329 (9)	−0.2729 (9)	0.1340 (5)
C(8a)	−0.6733 (9)	−0.2605 (9)	0.0919 (6)
C(9a)	−0.6912 (8)	−0.1341 (9)	0.0786 (5)
C(2b)	0.2087 (8)	0.3226 (8)	0.3051 (5)
C(4b)	0.3388 (8)	0.1776 (8)	0.3390 (5)
C(5b)	0.1876 (7)	0.1030 (7)	0.3043 (4)
C(6b)	0.1412 (8)	−0.0404 (8)	0.2961 (5)
C(7b)	0.2498 (9)	−0.1061 (9)	0.3221 (6)
C(8b)	0.4012 (9)	−0.0265 (10)	0.3571 (6)
C(9b)	0.4482 (8)	0.1153 (10)	0.3650 (6)
C(Me)	−0.1478 (11)	0.0727 (10)	0.4513 (6)
C(1)	−0.3484 (9)	0.3454 (8)	0.1563 (5)
C(2)	−0.1826 (8)	0.4191 (8)	0.1947 (5)
C(3)	0.0481 (10)	0.4674 (9)	0.3491 (6)
C(4)	0.1789 (9)	0.4568 (9)	0.2953 (6)

Table IV. Fractional Atomic Coordinates for Non-Hydrogen Atoms of $[Cu(BBES)(acac)]PF_6{\cdot}C_4H_8O_2$

atom	*x*	*y*	*z*
Cu	0.0101 (1)	0.2400 (1)	−0.1452 (2)
S(1)	−0.0911 (3)	0.3636 (3)	−0.2750 (4)
O(1a)	0.0431 (7)	0.1660 (7)	−0.3034 (11)
O(1b)	0.1480 (6)	0.3461 (8)	−0.0657 (10)
N(1a)	−0.1242 (8)	0.1146 (8)	−0.2132 (13)
N(1b)	−0.0158 (8)	0.3007 (9)	0.0357 (12)
C(1a)	−0.2025 (11)	0.2618 (11)	−0.4202 (15)
C(2a)	−0.1938 (12)	0.1442 (12)	−0.4494 (16)
N(2a)	−0.2862 (9)	0.0089 (10)	−0.3435 (15)
C(1b)	−0.1546 (11)	0.4110 (12)	−0.1525 (16)
C(2b)	−0.1879 (10)	0.3310 (13)	−0.0696 (16)
N(2b)	−0.0952 (9)	0.3552 (9)	0.1845 (13)
C(11a)	0.1359 (13)	0.1073 (14)	−0.4525 (20)
C(11b)	0.3280 (11)	0.4365 (15)	−0.0191 (18)
P(1)	0.4969 (4)	0.2080 (5)	−0.3187 (7)
F(1)	0.5798 (9)	0.1629 (12)	−0.2373 (18)
F(2)	0.5885 (8)	0.3126 (12)	−0.3116 (18)
F(3)	0.4129 (9)	0.2501 (13)	−0.4078 (18)
F(4)	0.4050 (9)	0.1010 (11)	−0.3313 (16)
F(5)	0.5081 (11)	0.1467 (14)	−0.4612 (17)
F(6)	0.4880 (11)	0.2692 (15)	−0.1785 (17)
C(3a)	−0.1994 (11)	0.0917 (12)	−0.3363 (16)
C(4a)	−0.2649 (12)	−0.0204 (13)	−0.2180 (18)
C(5a)	−0.3290 (14)	−0.0974 (14)	−0.1693 (19)
C(6a)	−0.2831 (15)	−0.1024 (15)	−0.0419 (21)
C(7a)	−0.1827 (14)	−0.0430 (14)	0.0439 (21)
C(8a)	−0.1215 (13)	0.0345 (13)	−0.0079 (18)
C(9a)	−0.1652 (11)	0.0450 (12)	−0.1363 (15)
C(3b)	−0.1000 (11)	0.3264 (12)	0.0462 (16)
C(4b)	−0.0039 (12)	0.3482 (13)	0.2640 (17)
C(5b)	0.0446 (14)	0.3710 (14)	0.4150 (20)
C(6b)	0.1371 (15)	0.3600 (15)	0.4585 (22)
C(7b)	0.1872 (14)	0.3270 (14)	0.3724 (20)
C(8b)	0.1426 (13)	0.2961 (14)	0.2209 (19)
C(9b)	0.0464 (11)	0.3147 (11)	0.1729 (16)
C(10a)	0.1342 (11)	0.1869 (12)	−0.3185 (16)
C(10b)	0.2248 (11)	0.3457 (12)	−0.1069 (16)
C(10c)	0.2230 (11)	0.2703 (11)	−0.2251 (15)
C(1s)	−0.3811 (11)	0.1535 (11)	0.1240 (17)
C(2s)	−0.3635 (11)	0.2705 (12)	0.2136 (16)
O(1s)	−0.2788 (12)	0.3428 (10)	0.2499 (15)
O(2s)	−0.4488 (11)	0.2887 (11)	0.2427 (16)
C(3s)	−0.4253 (12)	0.4001 (12)	0.3362 (16)
C(4s)	−0.5268 (13)	0.4205 (13)	0.3501 (18)

The crystal data are in Table II. No corrections for absorption were applied.

The structure was solved with use of the Patterson method and refined by blocked full-matrix least squares with complex neutral-atom scattering factors[17] and weights ($=1/[\sigma^2(F)]$) using the unique observed data ($I > 3\sigma(I)$), 2939 reflections) with the SHELX programs.[18a] The N–H hydrogen positions were obtained from a difference synthesis while the remaining H atom positions were estimated geometrically by using the spectroscopically determined C–H distance of 1.08 Å. The refined parameters included anisotropic thermal parameters for the heteroatoms. There was insufficient data to allow all the nonhydrogen atoms to be anisotropic; however, difference maps indicated residual electron density about the isotropic methyl and methylene C atoms, and consequently these atoms were included in the final cycles with anisotropic thermal parameters. The final R values were $R = 0.063$ and $R' (=\sum w^{1/2}\Delta/\sum w^{1/2}|F_o|)^{18b} = 0.061$ with 288 parameters and weights $w = 1/\sigma^2(F)$. The maximum residual electron density was 0.64 e/Å^3 in the region of the PF_6 anion. Final fractional atomic

---

(17) Cromer, D. T.; Mann, J. B. *Acta Crystallogr., Sect. A: Cryst. Phys., Diffr., Theor. Gen. Crystallogr.* **1968**, *A24*, 321.

(18) (a) Sheldrick, G. M. "SHELX 76 Program System"; Cambridge University: Cambridge, England, 1976. (b) Henrick, K.; McPartlin, M.; Deeming, A. J.; Hasso, S.; Manning, P. *J. Chem. Soc., Dalton Trans.* **1982**, 899.

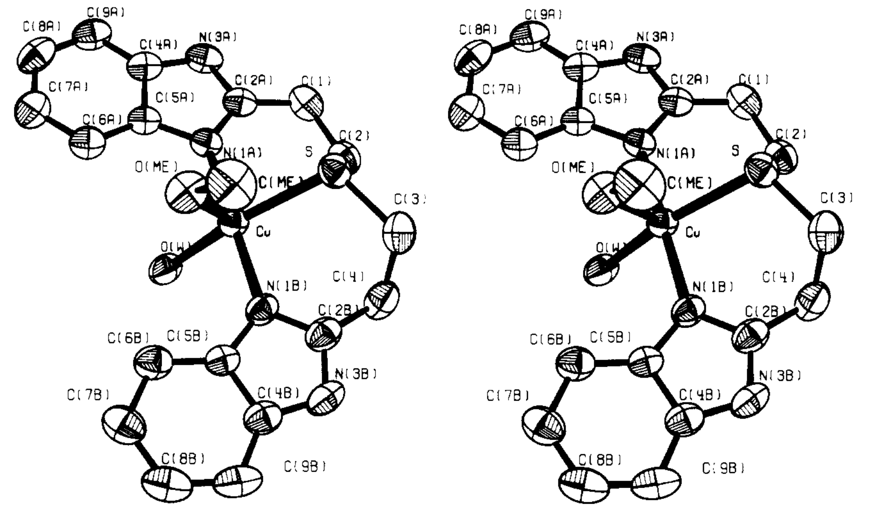

Figure 3. ORTEP stereoview of the structure of the cation $[\mathrm{Cu(BBES)(MeOH)(OH_2)}]^{2+}$ showing the atom-numbering scheme. Hydrogen atoms are omitted for clarity.

Table V. Selected Bond Lengths and Intermolecular Contacts (and Their Standard Deviations) (Å) in $[\mathrm{Cu(BBES)(MeOH)(OH_2)}](\mathrm{ClO_4})_2$[a]

Cu–S	2.297 (1)	C(2a)–C(1)	1.454 (6)
Cu–O(W)	1.995 (2)	C(4a)–C(5a)	1.403 (5)
Cu–O(Me)	2.261 (3)	C(4a)–C(9a)	1.367 (5)
Cu–N(1a)	1.984 (3)	C(2b)–C(4)	1.472 (6)
Cu–N(1b)	1.978 (3)	C(4b)–C(5b)	1.387 (5)
S–C(2)	1.818 (4)	C(4b)–C(9b)	1.379 (6)
S–C(3)	1.798 (4)	C(1)–C(2)	1.508 (6)
O(Me)–C(Me)	1.428 (5)	C(3)–C(4)	1.538 (6)
N(1a)–C(2a)	1.329 (4)	⟨$\mathrm{Cl_1}$–O⟩	1.342
N(1a)–C(5a)	1.385 (5)	⟨$\mathrm{Cl_2}$–O⟩	1.401
N(1b)–C(2b)	1.321 (5)	O(W)–O(5)($\mathrm{ClO_4^-}$)	2.800 (5)[a]
N(1b)–C(5b)	1.380 (5)	O(W)–O(5)($\mathrm{ClO_4^-}$)	2.860 (4)[b]
N(3a)–C(2a)	1.336 (5)	O(Me)–O(1)($\mathrm{ClO_4^-}$)	2.942 (6)[c]
N(3a)–C(4a)	1.351 (5)	O(2)–N(3b)	2.913 (7)[d]
N(3b)–C(2b)	1.342 (5)	O(5)($\mathrm{ClO_4^-}$)–N(3a)	2.927 (4)[e]
N(3b)–C(4b)	1.345 (5)	Cu–O(6)($\mathrm{ClO_4^-}$)	3.391 (3)[a]

[a] Symmetry transformations are given by the following superscripts: (a) x, y, z; (b) $-x, -y, -z$; (c) $-x, -y, 1-z$; (d) $1-x, 1-y, 1-z$; (e) $1+x, y, z$.

Table VI. Selected Bond Angles (and Their Standard Deviations) (deg) in $[\mathrm{Cu(BBES)(MeOH)(OH_2)}]^{2+}$

S–Cu–O(W)	158.6 (1)	Cu–N(1a)–C(5a)	123.8 (2)
S–Cu–O(Me)	94.8 (1)	C(2a)–N(1a)–C(5a)	105.8 (3)
S–Cu–N(1a)	86.3 (1)	Cu–N(1b)–C(2b)	126.7 (2)
S–Cu–N(1b)	95.2 (1)	Cu–N(1b)–C(5b)	127.3 (3)
O(W)–Cu–O(Me)	106.6 (1)	C–(2b)–N(1b)–C(5b)	105.9 (3)
O(W)–Cu–N(1a)	90.6 (1)	C(2a)–N(3a)–C(4a)	109.4 (3)
O(W)–Cu–N(1b)	86.1 (1)	C(2b)–N(3b)–C(4b)	110.5 (3)
O(Me)–Cu–N(1a)	93.0 (1)	N(1a)–C(2a)–N(3a)	111.0 (4)
O(Me)–Cu–N(1b)	92.1 (1)	N(1a)–C(2a)–C(1)	127.9 (3)
N(1a)–Cu–N(1b)	174.6 (1)	N(1b)–C(2b)–N(3b)	109.8 (4)
Cu–S–C(2)	95.4 (1)	N(1b)–C(2b)–C(4)	126.5 (4)
Cu–S–C(3)	108.8 (2)	C(2a)–C(1)–C(2)	117.7 (3)
C(2)–S–C(3)	101.2 (2)	S–C(2)–C(1)	108.6 (3)
Cu–O(Me)–C(Me)	120.8 (3)	S–C(3)–C(4)	115.8 (3)
Cu–N(1a)–C(2a)	130.4 (3)	C(2b)–C(4)–C(3)	112.8 (4)

Table VII. Selected Bond Lengths and Intermolecular Contacts (and Their Standard Deviations) (Å) in $[\mathrm{Cu(BBES)(acac)}]\mathrm{PF_6 \cdot C_4H_8O_2}$

Cu–S(1)	2.696 (5)	S(1)–C(1a)	1.828 (12)
Cu–O(1b)	1.918 (8)	O(1a)–C(10a)	1.289 (20)
Cu–N(1b)	2.006 (13)	N(1a)–C(3a)	1.331 (18)
S(1)–Cu(1b)	1.800 (18)	N(1b)–C(3b)	1.321 (22)
O(1b)–C(10b)	1.248 (20)	C(1a)–C(2a)	1.527 (23)
N(1a)–C(9a)	1.416 (21)	C(3a)–N(2a)	1.377 (19)
N(1b)–C(9b)	1.387 (18)	C(4a)–C(5a)	1.42 (3)
C(2a)–C(3a)	1.455 (25)	C(2b)–C(3b)	1.487 (21)
N(2a)–C(4a)	1.381 (24)	N(2b)–C(4b)	1.357 (21)
C(1b)–C(2b)	1.517 (25)	C(10a)–C(10c)	1.384 (16)
C(3b)–N(2b)	1.358 (21)	C(10b)–C(10c)	1.375 (21)
C(4b)–C(5b)	1.442 (25)	O(1s)–N(2b)	2.79
Cu–O(1a)	1.921 (11)	O(1s)–H(2nb)	2.05
Cu–N(1a)	1.996 (9)	F(5)–H(2na)	2.18[a]
		⟨P–F⟩	1.566

[a] Symmetry transformation $-x, -y, -1-z$.

coordinates are given in Table IV, while the important bond lengths and angles are listed in Tables VII and VIII. Fractional atomic coordinates for the hydrogen atoms and anisotropic thermal parameters are available as supplementary material.

Results and Discussion

Structural Aspects. Figure 2 is a stereoview of the unit cell contents of the simple Cu(BBES) perchlorate. As is evident from this, the structure consists of complex cations and relatively isolated perchlorate anions. The recently published[7] Cu(TMBBES) structure thus exhibits an unexpected difference compared to the coordination to be described here. In the crystals prepared by Dagdigian et al.,[7] only one of the two perchlorates is ionic, while the other is coordinated to the apical position of a roughly square-pyramidal cationic copper(II) complex. The alcohol (ethanol) which may be included in some crystals[9] appears not to coordinate.

On the other hand, substitution of ethanol[9] by methanol (this work) as the synthesis medium and demethylation of the rings lead to replacement of perchlorate by an alcohol molecule in the coordination sphere (Figure 3). This type of substitutional isomerism is an interesting feature of this benzimidazolyl–thioether system and is presumably subject to rather subtle control by lattice energy and solvation free energies in various solvents.

Substitution of an anionic by a neutral ligand should increase the Lewis acidiity of the copper center. Indeed, the equatorial bonds average 0.014 (2) Å shorter in the methanol than in the perchlorato complex, only one bond (Cu–N(2)) being 0.018 (4) Å longer. The S atom moves 0.025 (2) Å closer, while the equatorial water molecule moves inward by 0.050 (3) Å.

In both structures, the axial Cu–O bond is intrinsically the longest (making allowance for the different atomic sizes of O and S), though the uncharged methanol oxygen is bound 0.09 Å closer than the perchlorato oxygen, a perhaps counterintuitive result.

In both $[\mathrm{Cu(TMBBES)(ClO_4)(OH_2)}]^+$ and $[\mathrm{Cu(BBES)(MeOH)(OH_2)}]^{2+}$, the meridional BBES ligand's donor atoms are all coordinated equatorially, with the benzimidazole nitrogens mutually trans, and an oxygen is coordinated axially

Table VIII. Selected Bond Angles (and Their Standard Deviations) (deg) in $[Cu(BBES)(acac)]^+$

O(1a)–Cu–S(1)	98.2 (3)	O(1b)–Cu–S(1)	99.3 (3)
O(1b)–Cu–O(1a)	91.8 (4)	N(1a)–Cu–S(1)	89.4 (4)
N(1a)–Cu–O(1a)	87.3 (5)	N(1a)–Cu–O(1b)	171.4 (5)
N(1b)–Cu–S(1)	90.8 (4)	N(1b)–Cu–O(1a)	170.8 (5)
N(1b)–Cu–O(1b)	88.0 (4)	N(1b)–Cu–N(1a)	91.5 (5)
C(1a)–S(1)–Cu	104.8 (5)	C(1b)–S(1)–Cu	102.7 (6)
C(1b)–S(1)–C(1a)	101.2 (7)	C(10a)–O(1a)–Cu	125.8 (8)
C(10b)–O(1b)–Cu	127.5 (8)	C(3a)–N(1a)–Cu	125 (1)
C(9a)–N(1a)–Cu	128.2 (8)	C(9a)–N(1a)–C(3a)	106 (1)
C(3b)–N(1b)–Cu	126 (1)	C(9b)–N(1b)–Cu	127 (1)
C(9b)–N(1b)–C(3b)	107 (1)	C(2a)–C(1a)–S(1)	113 (1)
C(3a)–C(2a)–C(1a)	115 (1)	C(2a)–C(3a)–N(1a)	126 (1)
N(2a)–C(3a)–N(1a)	110 (1)	N(2a)–C(3a)–C(2a)	123 (1)
C(4a)–N(2a)–C(3a)	108 (1)	C(2b)–C(1b)–S(1)	115 (1)
C(3b)–C(2b)–C(1b)	114 (1)	C(2b)–C(3b)–N(1b)	128 (1)
N(2b)–C(3b)–N(1b)	110 (1)	N(2b)–C(3b)–C(2b)	122 (1)
C(4b)–N(2b)–C(3b)	108 (1)	C(10c)–C(10a)–O(1a)	125 (1)
C(11a)–C(10a)–O(1a)	113 (1)	C(11a)–C(10a)–C(10c)	122 (1)
C(10c)–C(10b)–O(1b)	125 (1)	C(11b)–C(10b)–O(1b)	117 (1)
C(11b)–C(10b)–C(10c)	118 (1)	C(10b)–C(10c)–C(10a)	124 (1)

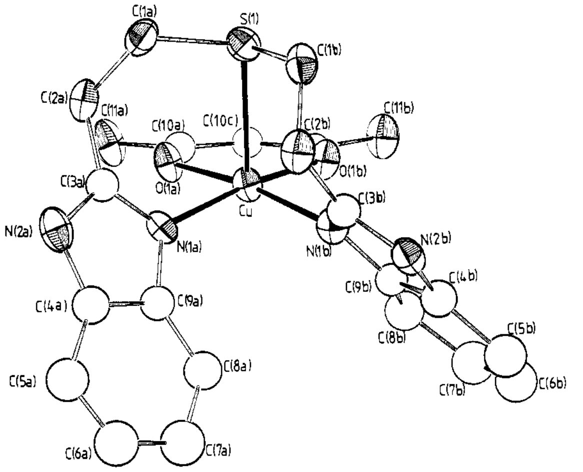

Figure 4. Structure of $[Cu(BBES)(acac)]^+$ showing the atom-numbering scheme. Hydrogen atoms are omitted for clarity.

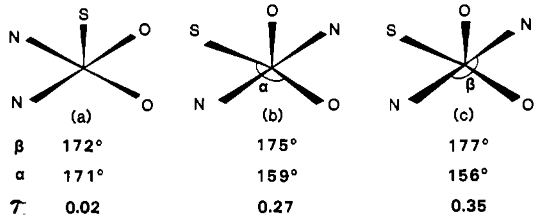

Figure 5. Relative coordination geometries and τ-defining angles α, β in (a) $[Cu(BBES)(acac)]^+$, (b) $[Cu(BBES)(MeOH)(OH_2)]^{2+}$, and (c) $[Cu(BBES)(ClO_4)(OH_2)]^+$ (from ref 7). $\tau = (\beta - \alpha)/60$.[12]

Table IX. Structural Indices for Selected N,S-Donor Copper(II) Complexes

species	donor set	τ	ref
$[Cu(BBES)(acac)]^+$	N_2SO_2	0.01	this work
$[Cu(pdto)(ClO_4)]^{+\,a}$	N_2S_2O	0.12	5
$[Cu(BBES)(MeOH)(OH_2)]^{2+}$	N_2SO_2	0.27	this work
$[Cu(BBES)(ClO_4)(OH_2)]^{+\,b}$	N_2SO_2	0.34	7
$[Cu(Me_2BBDHp)(OH_2)]^{2+}$	N_2S_2O	0.48	12
$[Cu(bbtb)(OH_2)]^{2+}$	$N_2S_2O^c$	0.65	6

[a] pdto is 1,8-bis(2-pyridyl)-3,6-dithiaoctane. [b] Me_2BBDHp is 1,7-bis(benzimidazol-2-yl)-2,6-dithiaheptane. [c] bbtb is *o*-phenylenebis(benzimidazol-2-yl methyl sulfide).

to the copper. On the other hand, in the similarly pentacoordinate $[Cu(BBES)(acac)]^+$, the N_2O_2S donor set is isomeric (Figure 4) so that the now-folded BBES ligand is facially coordinated and presents its nitrogens cis to the metal's equator, the thioether sulfur thus being axially coordinated. This displacement of the thioether sulfur from an equatorial to the axial position is accompanied by a Cu–S bond length increase of 0.40 Å, to 2.70 Å. The latter value falls within the usual range for apical Cu–S(thioether) bonds.[7,19]

The set of complexes $[Cu(BBES)(MeOH)(OH_2)]^{2+}$, $[Cu(TMBBES)(ClO_4)(OH_2)]^+$, and $[Cu(BBES)(acac)]^+$ thus entail the interesting situation of having the thioether sulfur occupy the two site extremes possible within what is essentially axial-tetragonal type coordination geometry, with the same primary ligand type (BBES). This situation is very similar to that recently explored by Schugar et al., with substituted imidazoyl–thioether ligands,[19] where relative donor atom positioning was imposed by appropriate ligand architecture.

A possible rationale for the observed isomer preference by $[Cu(BBES)(acac)]^+$ is suggested by the fact that of the 15 copper–ligand bonds in the three BBES-type complexes the two Cu–O(acetylacetonate) ones are the shortest. Relative to the other ligands, this suggests that these oxygens may be the strongest donors and with the Cu atom will thus define the equatorial *xy* plane, rather than one of them defaulting to a more weakly bound *z*-axial position (as in the alternative N_2OS equatorial isomer). Because thioether ligands are weaker donors,[20] the sulfur, rather than nitrogen, is displaced to the axial position as a consequence. The results of competition between heterocyclic nitrogen and β-keto enolate oxygen are not as clear-cut.[21]

The coordination is of course not precisely square-pyramidal in either of the complexes reported here (Figure 5). However, allowing for the heterogeneous donor sets, and for the fact that the metal is usually raised above the basal plane of a square pyramid,[22,23] one can, amongst these complexes, explore the degree of distortion away from the tetragonal pyramidal toward the trigonal bipyramidal. To do this, we use the geometric index τ, which describes the position of a pentacoordinate centric molecule along the continuum between the above two extreme geometries.[12] For $[Cu(BBES)(acac)]^+$, $\tau = 0.02$, so the donor atom array of this cation is very close to being perfectly tetragonal (Table IX), with the Cu atom 0.15 Å above the basal N_2O_2 plane. The N(1)–Cu–N(3) and

---

[19] Prochaska, J. J.; Schwindinger, W. F.; Schwartz, M.; Burk, M. H.; Bernarducci, E.; Lalancette, R. A.; Potenza, J. A.; Schugar, H. J. *J. Am. Chem. Soc.* **1981**, *103*, 3446.

[20] Murray, S. G.; Hartley, F. R. *Chem. Rev.* **1981**, *81*, 365.

[21] (a) Bushnell, G. W. *Can. J. Chem.* **1971**, *49*, 55. (b) Ooi, S.; Fernando, Q. *Chem. Commun.* **1967**, 532.

[22] Hathaway, B. J.; Hodgson, P. G. *J. Inorg. Nucl. Chem.* **1973**, *35*, 4071.

[23] Hoskins, B. F.; Whillans, F. D. *Coord. Chem. Rev.* **1972**, *9*, 365.

[24] The C atoms of the ester solvate in $Cu(BBES)(acac)(PF_6)(C_4H_8O_2)$ are numbered 1s–4s from left to right in the formula $CH_3C(O)OCH_2CH_3$, and the carbonyl O is O(1s).

Table X. Electron Spin Resonance Data[a]

compd	medium	g_0	-10^4A_0	$g_\parallel$	$-10^4A_\parallel$	$g_\perp$	$-10^4A_\perp$
$[Cu(BBES)(MeOH)(OH_2)](ClO_4)_2$	$MeNO_2$	2.109	≤29[b]	2.223	146	2.06	≤−30
$[Cu(BBES)(MeOH)(OH_2)](ClO_4)_2$	MeOH/acetone	2.122	≤26[b]	2.234	151	2.06	≤−37
$[Cu(BBES)(MeOH)(OH_2)](ClO_4)_2$	DMF[c]	2.14	40	2.246 (A) 2.35 (B)	140 (A) 140 (B)		−10
$[Cu(BBES)_2]^{2+}$	DMF			2.264	185	2.06	
$[Cu(bpy)(acac)]ClO_4{\cdot}MeOH$	$MeOH/MeNO_2$	2.119	74	2.253	189	2.06	17
$[Cu(Pmeta)(acac)]ClO_4$	MeOH/acetone	2.129	61	2.239	170	2.07[d]	7
$[Cu(BBES)(acac)]PF_6{\cdot}H_2O{\cdot}EtOH$	$MeNO_2$	2.128	72	2.264	187	2.06	15
$[Cu(BBES)(acac)]PF_6{\cdot}H_2O{\cdot}EtOH$	DMF	2.134	74	2.284	178	2.06	22
$[Cu(Me_2BBEO)_2](ClO_4)_2{\cdot}H_2O$	acetone/toluene	2.149	76	2.284	168	2.06	30
$[Cu(Me_2BBEO)_2](ClO_4)_2{\cdot}H_2O$	neat powder			2.274	184	2.05	
$[Cu(Me_2BBEO)]^{2+}$	$MeOH/MeNO_2$[e]	2.143	≤20[b]	2.346	133	2.08	≤−37

[a] Values determined as described in the Experimental Section; g_0, $g_\parallel$ ±0.003, $g_\perp$ ±0.01, A values in cm^{-1}. [b] One-third of the width between the first-derivative spectrum's maximum and minimum. [c] The values are of lower precision than above, because of overlapping spectral features. [d] $g_\perp = \frac{1}{2}(3g_0 - g_\parallel)$. [e] There is a second species present.

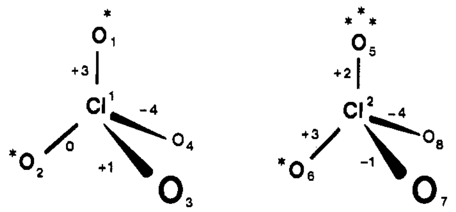

Figure 6. Perchlorate anions of $[Cu(BBES)(MeOH)(OH_2)](ClO_4)_2$, indicating the numbering scheme. The signed values indicate length differences (in pm) from that ion's mean Cl–O bond length. Asterisks denote that a cationic moiety (H or Cu) is nearby.

S–Cu–O(w) angles in the ((TM)BBES)Cu^{II} perchlorates are roughly similar; both complexes are about 30% distorted toward the trigonal-bipyramidal state, the perchlorato complex a little more so than the methanol adduct, as judged by the τ values.

It is worth noting, at this point, that structural variation about the copper(II) appears to occur in a quite facile fashion with these thioether–benzimidazole systems; the small τ variation seen for the above perchlorates appears on a grander scale in perchlorates of the copper(II) complex of Me_2BBDHp[12] (1,7-bis(benzimidazol-2-yl)-2,6-dithiaheptane, Table IX).

There are hydrogen-bonding interactions in both $[Cu(BBES)(MeOH)(OH_2)](ClO_4)_2$ and the ethyl acetate solvate of $[Cu(BBES)(acac)](PF_6)$.

In $[Cu(TMBBES)(ClO_4)(OH_2)](ClO_4)$, the equatorial water was reported to be H bonded to the noncoordinated perchlorate[7] and a similar situation exists in $[Cu(BBES)(MeOH)(OH_2)]{:}ClO_4)_2$, where O(5)'s of two crystallographically equivalent perchlorates 2 are at 2.80 and 2.86 Å from the coordinated water's oxygen (Table V). These perchlorate oxygens appear to be nested in a potential well associated also with benzimidazole pyrrolyl N–H (Table V, Figure 6). Other H-bonding attractions seem likely, from pyrrolyl N–H and methanolic O–H to perchlorate 1. The longest Cl–O bond is that for which the oxygen atom O(6) is electrostatically aligned with its nearest neighbor, the copper cation, though the interaction is too distant to be considered coordinative (Table V).

In $[Cu(BBES)(acac)]PF_6{\cdot}C_4H_8O_2$, the hydrogen-bonding network (Figure 7) is further removed from the coordinating atoms. Again, the pyrrolyl nitrogens of the benzimidazole rings are involved, one interacting with a hexafluorophosphate anion, the other with the ethyl acetate carbonyl oxygen (Table VII).

Distances and angles within the acetylacetonate ligand are comparable to those previously reported.[21,25,26] The benzimidazole groups show no unusual features, and their geometries are in agreement with previously reported structures.[6,27] For example, they are planar to within ca. 0.02 Å in $[Cu(BBES)(acac)]^+$.

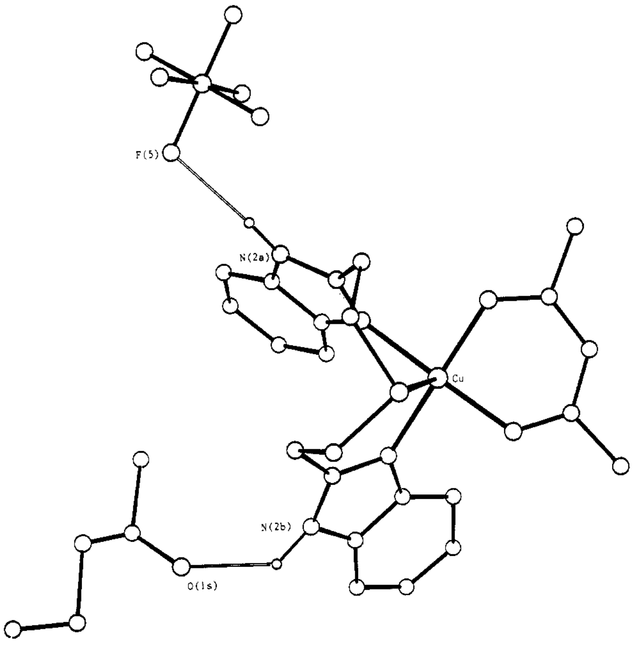

Figure 7. Hydrogen-bonding network in $[Cu(BBES)(acac)]PF_6{\cdot}C_4H_8O_2$. The upper benzimidazole ring is ring A.

The benzimidazole rings in $[Cu(BBES)(acac)]^+$ are inclined in a like sense to the CuN_2O_2 plane by angles of 54.6° (ring A) and 53.0° (ring B), this twist being roughly the same as in tetrakis(*N*-methylimidazole)copper(II) perchlorate.[28]

Electron Spin Resonance Spectra and Cryogenic Solution Chemistry. Both of the structurally characterized compounds show behavior that is not straightforward in all circumstances.

Nonetheless, the *N*,*N*-dimethylformamide (DMF) and nitromethane solutions of $[Cu(BBES)(acac)]^+$ generally have the higher $g_\parallel$ and $A_\parallel$ values at 77 K (Table X). These data, as well as those for $Cu(Me_2BBEO)^{2+}$ and $[Cu(bpy)(acac)]^+$, lie clearly in the region associated with an N_2O_2 equatorial donor atom set in an $A_\parallel$–$g_\parallel$ plot.[10,29,30]

If equatorial oxygen is replaced by a sulfur donor, the value of $g_\parallel$ should decrease, and indeed $g_\parallel$ for $[Cu(BBES)]^{2+}$ in

---

(25) Piper, T. S.; Belford, R. L. *Mol. Phys.* **1962**, *5*, 169.

(26) Robertson, I.; Truter, M. R. *J. Chem. Soc. A* **1967**, 309.

(27) Hendriks, H. M. J.; Birker, P. J. M. W. L.; van Rijn, J.; Verschoor, G. C.; Reedijk, J. *J. Am. Chem. Soc.* **1982**, *104*, 3607.

(28) Ivarsson, G. *Acta Chem. Scand., Ser. A* **1973**, *27*, 3523.

(29) Peisach, J.; Blumberg, W. E. *Arch. Biochem. Biophys.* **1974**, *165*, 691.

(30) Addison, A. W. In "Copper Coordination Chemistry: Biochemical and Inorganic Perspectives"; Karlin, K. D., Zubieta, J. A., Eds.; Adenine Press: Guilderland, NY, 1983; p 109.

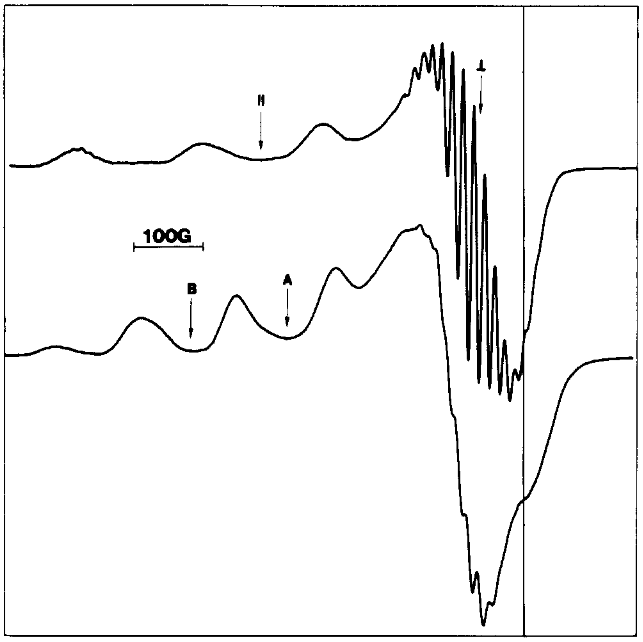

Figure 8. 77K X-band ESR spectra of [Cu(BBES)(MeOH)(OH_2)]$(ClO_4)_2$, in MeOH–acetone (lower) and in DMF with excess BBES added (upper). The arrows denote the $g_{\|}$ values of species A and B (Table X), while the vertical line marks $g = 2$.

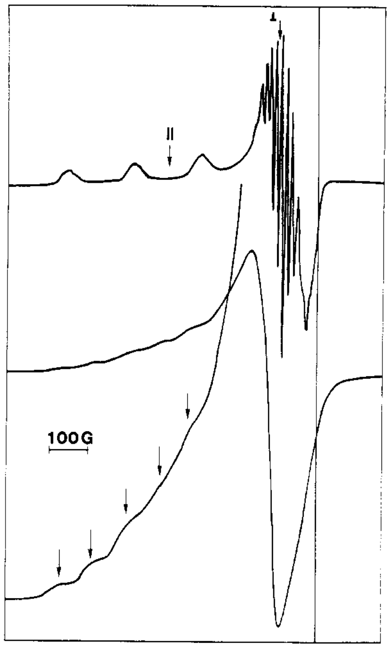

Figure 9. X-Band ESR spectra of [Cu(BBES)(acac)]PF_6·H_2OEtOH as (upper) a $MeNO_2$–TEOF solution at 77 K and (lower) a pure powder at ambient temperature, with 25× gain increase displayed for the lower field region. The vertical line marks $g = 2$. The field span is twice that of Figure 8.

nitromethane or acetone–methanol is significantly less (by 0.02–0.05). The $g_{\|}$, $A_{\|}$ data for the nitromethane solution in particular seem quite indicative of thioether sulfur in the equatorial plane while indicating also that the complex remains distorted from the tetragonal in this solvent. In fact, the spectra are not perfectly axial but appear to be slightly rhombic in solution (Figure 8, lower spectrum). The generally more distorted coordination for $Cu(BBES)^{2+}$ and $Cu(Me_2BBEO)^{2+}$ is also suggested by the positive values deduced for $A_{\perp}$, a phenomenon which has also been noted for tetracoordinate copper(II).[31] This sign difference between $A_{\|}$ and $A_{\perp}$ leads to unusually small A_0 values for $Cu(BBES)^{2+}$ and $Cu(Me_2BBEO)^{2+}$ so that, at ambient temperatures, their fluid-solution spectra in $MeNO_2$ or MeOH–acetone consist of a single line with no hyperfine splitting.

In the DMF solution spectrum of $Cu(BBES)^{2+}$, two species are clearly observed at 77K; this was also noted by Dagdigian et al.[7] A lesser amount of the higher $g_{\|}$-value species ("B", Table X) is evident in the methanol–acetone glass as well (Figure 8). In fact, the cryogenic solution chemistry bears further consideration.

There are potentially three equilibria that could be operating to yield the two species:

$$mer\text{-}Cu(BBES)S_x^{2+} \rightleftharpoons fac\text{-}Cu(BBES)S_x^{2+} \quad (1)$$

$$Cu(BBES)S_x^{2+} \rightleftharpoons BBES + CuS_y^{2+} \quad (2)$$

$$2Cu(BBES)S_x^{2+} \rightleftharpoons CuS_y^{2+} + Cu(BBES)_2^{2+} \quad (3)$$

where the meridional and facial isomers correspond to equatorial and axial sulfur, respectively, and S represents other solute/solvent donor molecules.

The simple dissociation process (2) is ruled out, because the ESR spectrum of [Cu(BBES)(MeOH)(OH_2)]$(ClO_4)_2$ in DMF is independent of concentration and because the lower field species has a $g_{\|}$ value different from that of copper(II) perchlorate in DMF ($g_{\|} = 2.392$, $A_{\|} = 137$). The latter fact also disfavors the disproportionation process (3), although disproportionation of thioether complexes of copper(II) is a common problem.[32] Furthermore, addition of excess BBES ligand gives rise to an entirely new set of resonances (Figure 8). The N-shf structure in the $g_{\perp}$ region clearly shows this to have a N_4(heterocyclic) donor set (contrast Figure 9) and thus identifies $[Cu(BBES)_2]^{2+}$, with sulfurs mutually trans on the axial directions.

It appears that the distinct N-shf structure associated with equatorial nitrogen is lost when the structure loses tetragonality (e.g. $[Cu(BBES)_2]^{2+}$) and becomes more trigonal (e.g. $Cu(BBES)^{2+}$), as well as when heterocyclic nitrogen is replaced by aliphatic nitrogen;[10] there is no N-shf visible for $[Cu(pmeta)(acac)]^+$.

These results overall indicate that the two cryogenic-solution species observed for $Cu(BBES)^{2+}$ in DMF are isomeric with respect to BBES coordination, the predominant ($g_{\|} = 2.246$) complex being the meridional isomer.[33]

The nitromethane–TEOF[34] solution spectrum of [Cu(BBES)(acac)]PF_6·H_2O·EtOH (Figure 9) is a fairly typical axial-tetragonal type of spectrum, with eight well-resolved lines in the high-field region, associated with $A_{\perp}$(Cu) and A(N) from two heterocyclic nitrogens. We note (Table X) the $g_{\|}$, $A_{\|}$ coincidence with $[Cu(BBES)_2]^{2+}$, but this is not unexpected.[10,30] The solution spectra of $Cu(Me_2BBEO)(ClO_4)_2$ and $[Cubpy)(acac)]^+$ are both similar to that of $[Cu(BBES)(acac)]^+$, while those of $[Cu(BBES)_2]^{2+}$ and $[Cu(Me_2BBEO)_2]^{2+}$ are, of course, virtually identical in appearance.

Attempts to obtain the spectrum of $[Cu(Me_2BBEO)(acac)]^+$ by addition of Na(acac) to $Cu(Me_2BBEO)^{2+}$ in methanol–acetone yielded the spectra of $[Cu(Me_2BBEO)_2]^{2+}$ and $Cu(acac)_2$, superimposed in an equimolar ratio at 77 K. This evidences the complete disproportionation of the mixed-ligand complex.

Among the solid-state spectra, only those of [Cu(BBES)(acac)]PF_6 and $[Cu(Me_2BBEO)_2](ClO_4)_2$·$H_2O$ are

---

[31] Yokoi, H.; Addison, A. W. *Inorg. Chem.* **1977**, *16*, 1341.

[32] Addison, A. W.; Rao, T. N.; Sinn, E., submitted for publication.

[33] We have no evidence that $Cu(BBES)_2^{2+}$ is stable toward ligand dissociation at ambient temperature, particularly in DMF.

[34] TEOF = triethyl orthoformate.

Table XI. Electronic Absorption Spectra Assignments, λ (ε)[a] at Ambient Temperature

chromophore	solvent	d–d	charge transfer	ligand $\pi \rightarrow \pi^*$, n $\rightarrow \pi^*$
BBES	MeOH			280 (8140, sh), 273 (9300), 245 (11 600), 217 (8800)
Me_2BBEO	MeOH			280 (8370), 273 (11 500), 250 (12 300), 215 (11 700)
biim	0.01 M HCl			275 (15 600)
$[Cu(pmeta)(acac)]ClO_4$	MeOH	790 (221)	265 (19 700)	302 (19 700)
$[Cu(bpy)(acac)]ClO_4 \cdot MeOH$	MeOH	590 (70)		307 (18 400, sh), 298 (23 900), 240 (14 100)
$[Cu(BBES)(MeOH)(OH_2)](ClO_4)_2$	MeOH	710 (180)	335 (1700)	277 (13 200), 270 (16 400), 241 (14 800)
$Cu(Me_2BBEO)^{2+}$ [b]	MeOH	695 (65)	353 (260)	279 (16 500), 273 (20 700), 245 (18 900)
$[Cu(Me_2BBEO)_2](ClO_4)_2 \cdot H_2O$	MeOH	635 (150)[c]	337 (590),[c] 304 (885)[d]	279 (20 300), 275 (28 300), 255 (25 000)
$[Cu(BBES)(acac)]PF_6 \cdot H_2O \cdot EtOH$	MeCN	690 (63), 590 (65)		302 (9240),[e] 277 (17 000), 270 (17 000), 240 (17 000)
$[Cu(BBES)(acac)]PF_6 \cdot H_2O \cdot EtOH$ vs. $[Cu(pmeta)(acac)]ClO_4$ [f]	MeOH	*g*	345 (1500), 320 (−1670)	302 (6800)
$Cu(BBES)^{2+}$ vs. $Cu(Me_2BBEO)^{2+}$ [b,f]	MeOH	690 (112)	420 (100, sh), 335 (1300)	

[a] λ in nm, ε in L mol^{-1} cm^{-1}. [b] Equimolar $Cu(ClO_4)_2 \cdot 6H_2O$ and Me_2BBEO in MeOH. [c] Excess Me_2BBEO added. [d] Not assigned. [e] Includes S/Cu LMCT. [f] Difference spectrum, (sulfur system) – (nonsulfur system); intensity given is Δε value. [g] Δε negative throughout d–d region.

informative, and they are somewhat unusual. First, the lattice of the latter salt is magnetically dilute, so that the parallel region Cu-hyperfine structure is clearly resolved in the neat powder at ambient temperature (Table X). Secondly, there is fine structure resolved on the low-field sides of the resonances for the neat powders of both the hydrate (Figure 9) and the ester solvate of $[Cu(BBES)(acac)]PF_6$, suggesting again that their lattices are also magnetically dilute. This is not unreasonable, if one considers that, in the ethyl acetate solvate, there are no bonding interactions even indirectly linking the complex cations (Figures 7 and 10) and that the shortest Cu–Cu distance is 7.346 Å. However, the spacings between the hyperfine lines in Figure 9 average only 86 G, about half the solution $a_{\parallel}$ value. This fact and the presence of a very weak resonance associable with a $\Delta M_s = 2$ transition indicate that the $[Cu(BBES)(acac)]^+$ molecules are pairwise interacting in the solid state. This must be attributed to a dipolar spin–spin interaction,[35] in the absence of evidence for another coupling pathway. This triplet-state fine structure is not as well resolved in the ester solvate as it is in $[Cu(BBES)(acac)]PF_6 \cdot H_2O \cdot EtOH$. In the ester solvate lattice, a simple dipolar coupling model[36] predicts $D = 0.0084$ cm^{-1} for $r(Cu–Cu) = 7.346$ Å. Coincidentally, a similar coupling pattern appears putatively in the spectrum of polycrystalline $[Cu(bpy)(acac)]ClO_4 \cdot MeOH$, where three parallel region features separated by about 100 G are distinguishable. In the $[Cu(BBES)(acac)]PF_6 \cdot H_2O \cdot EtOH$ spectrum (Figure 9) the fourth line observed is likely to be the central one of the seven-line triplet-state spectrum; its field position ($g = 2.279$) corresponds closely to the solution $g_{\parallel}$ value (Table X).

Finally, we note that there are significant differences between the $g_{\parallel}$ values reported here for $Cu(BBES)^{2+}$ and those reported previously[7] for this and similar complexes. We are uncertain as to the source of this variation.

Electronic Absorption Spectra and Ambient-Temperature Chemistry. The absorption spectra of the ligands, both free and coordinated, are dominated by their internal $\pi \rightarrow \pi^*$ transitions[37] in the ultraviolet region (Table XI).

The ligand field strength of thioether donors is intermediate between that of oxygen and heterocyclic nitrogen,[38] so that a square N_2O_2 or N_2OS donor array might be expected to produce a d–d manifold in the region 550–600 nm. The considerably longer wavelengths observed (Table XI) are a clear indication of the strong interaction of an additional axial (or pseudoaxial) ligand in all the systems.[11,39]

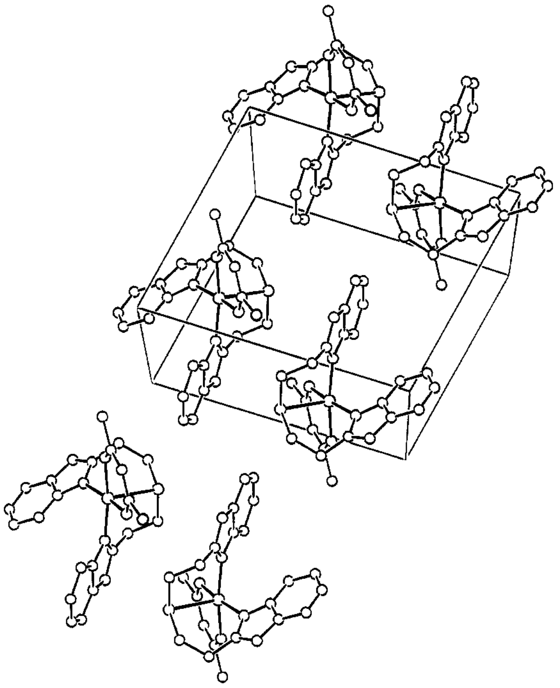

Figure 10. Packing diagram of $[Cu(BBES)(acac)]PF_6 \cdot C_4H_8O_2$. Hydrogen atoms, ester molecules, and anions are omitted for clarity.

In passing from the regular tetragonal structure of $[Cu(BBES)(acac)]^+$, with its axial thioether sulfur, to the more distorted $Cu(BBES)^{2+}$ chromophore, with its pseudoequatorial sulfur donor, one may note that the visible region absorption is generally enhanced in intensity.

In the near-UV, such a comparison is complicated by the presence of strong absorption at 302 nm, due to the acetylacetone ligand's $\pi_3 \rightarrow \pi_4$ transition[40] in the former complex.

---

(35) Addison, A. W.; Burke, P. J.; Henrick, K. *Inorg. Chem.* **1982**, *21*, 60.

(36) Yokoi, H. *Chem. Lett.* **1973**, 1023.

(37) Mason, S. F. In "Physical Methods in Heterocyclic Chemistry"; Katritzky, A. R., Ed.; Academic Press: New York, 1963; Vol. II, Chapter 7.

(38) Kauffman, G. B.; Tsai, J. H.-S.; Fay, R. C.; Jørgensen, C. K. *Inorg. Chem.* **1963**, *2*, 1233.

(39) Addison, A. W.; Carpenter, M.; Lau, L. K.-M.; Wicholas, M. *Inorg. Chem.* **1978**, *17*, 1545.

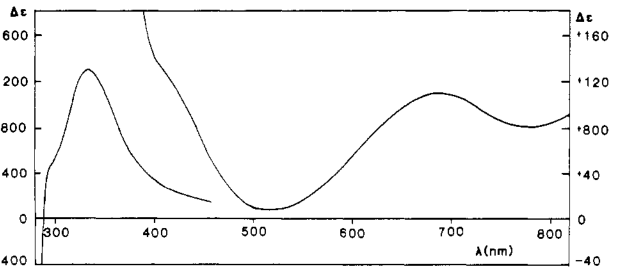

Figure 11. UV–visible difference spectrum (MeOH, 300 ± 2 K), with $Cu(BBES)^{2+}$ in the sample beam and $Cu(Me_2BBEO)^{2+}$ in the reference beam.

For this reason, we sought to isolate the acac-derived absorptions by synthesizing mono(acetylacetonate) chromophores of the type $LCu(acac)^+$, where L does not include sulfur. With L = bpy, there are coordination-enhanced transitions associated with the bpy ligand that tail significantly beyond 300 nm. The ligand 2,2′-biimidazole has its UV absorptions at shorter wavelength, but unlike $[Cu(bpy)(acac)]^+$,[41] the $[Cu(biim)(acac)]^+$ complex tends to disproportionate, yielding $Cu(biim)_2^{2+}$ [10] and other products. The same appears to be true for $[Cu(Me_2BBEO)(acac)]^+$, as attempts to synthesize its perchlorate salt have so far yielded only $[Cu(Me_2BBEO)_2](ClO_4)_2$. The effect on the UV absorptions of the relocation of the equatorial sulfur to the axial position in these systems is thus unclear. Direct comparison of $[Cu(BBES)(acac)]^+$ with the nonsulfur model compound $[Cu(pmeta)(acac)]^+$ via difference spectrophotometry reveals a broad absorption in the former at 345 nm (Table XI), which is probably associated with $N(\pi) \rightarrow Cu$ charge transfer (vide infra). However, the $acac^-$-derived absorptions of $[Cu(BBES)(acac)]^+$ are not well canceled by $[Cu(pmeta)(acac)]^+$ (e.g., negative ϵ, Table IX).

Isolation of the effects on the optical spectra, of the *presence* of the BBES sulfur is rather more straightforward, as the 1:1 Me_2BBEO:Cu(II) complex provides a direct comparison. The visible–UV difference spectrum (Table XI, Figure 11) shows that there is absorbance enhancement by sulfur over the whole observation range (300–800 nm), even though the $O \rightarrow S$ replacement is expected to shift the d–d bands.[42] The strong band (ϵ = 1300) at 335 nm is thus most likely associated with sulfur–copper LMCT,[7,43] and we assign it as $S(\sigma) \rightarrow Cu(d)$. This assignment agrees with that of previous work on related systems.[7] Other workers[43] have assigned considerably longer wavelength absorption bands as characteristic of $S(\sigma) \rightarrow Cu(d)$, but the observed wavelength is in general dependent on the coordination geometry and the other donors present.[7,43,44]

A complementary $S(\pi) \rightarrow Cu(d)$ transition, which has lesser intensity and is shifted to lower energy by 5000–7000 cm^{-1}, has been proposed to occur.[43] In Figure 11, there is a shoulder near 420 nm, which fits this criterion. The enhanced intensity around 700 nm would then be attributed to intensity borrowing[45] from the CT region.

Other bands, attributable to $N(\pi) \rightarrow Cu(d)$,[19] are also observed, notably in the 350-nm region in the Me_2BBEO complexes, where ether- and thioether-related transitions can be ruled out. In addition, in the $(Me_2BBEO)_2$ complex, a new absorption arises at 304 nm, which is not present in the 1:1 systems.

Conclusions. The results presented here support the conclusion[12] that copper(II) stereochemistry is relatively facultative when the donor set is composed of heterocyclic nitrogen and thioether sulfur. The biomimetic nature of these donors suggests, in turn, the likelihood that the energetic constraints on the stereochemistry of similarly ligated protein copper(II) are minimal.

By contrast, introduction of a strong σ donor (acetylacetonate) causes the coordination sphere to become distinctly more tetragonal in these systems, where ligand stereochemistry doe not itself force trigonal symmetry on the copper(II).

The present study also provides clear evidence for the $S \rightarrow Cu$ charge-transfer nature of the absorption bands near 330 nm in thioether complexes of copper(II).

Acknowledgment. We thank N. Amin for assistance with NMR spectra, Drexel University for research support, and Prof. F. Urbach for helpful discussion.

Registry No. Me_2BBEO, 87372-80-3; $[Cu(pmeta)(acac)]ClO_4$, 87372-86-9; $[Cu(bpy)(acac)]ClO_4$, 67360-85-4; $[Cu(BBES)(MeOH)(OH_2)](ClO_4)_2$, 87372-82-5; $[Cu(Me_2BBEO)]^{2+}$, 87372-88-1; $[Cu(Me_2BBEO)_2](ClO_4)_2$, 87372-84-7; $[Cu(BBES)(acac)]PF_6 \cdot H_2O \cdot EtOH$, 87393-38-2; $[Cu(BBES)_2]^{2+}$, 87372-87-0; bis(2-cyanoethyl) ether, 1656-48-0; *N*-methyl-*o*-phenylenediamine, 4760-34-3.

Supplementary Material Available: Fractional atomic coordinates and anisotropic thermal parameters (Table XII), bond lengths (Table XIII), bond angles (Table XIV), and observed and calculated structure factors (Table XV) for $[Cu(BBES)(MeOH)(OH_2)](ClO_4)_2$, fractional atomic coordinates for hydrogen atoms (Table XVI), anisotropic thermal parameters (Table XVII), bond lengths (Table XVIII), bond angles (Table XIX), intermolecular distances (Table XX), intramolecular distances (Table XXI), least-squares planes and deviations therefrom (Table XXII), and observed and calculated structure factors (Table XXIII) for $[Cu(BBES)(acac)](PF_6) \cdot C_4H_8O_2$, and least-squares planes and deviations therefrom for $[Cu(BBES)(MeOH)(OH_2)](ClO_4)_2$ (Table XXIV) (50 pages). Ordering information is given on any current masthead page.

---

(40) Johnson, R. R.; Thornton, D. A. *J. Mol. Struct.* **1975**, *29*, 97.

(41) (a) Doraswamy, U.; Bhattacharya, P. K. *Indian J. Chem.* **1975**, *13*, 1069. (b) Fukuda, Y.; Sone, K. *Bull. Chem. Soc. Jpn.* **1970**, *43*, 556.

(42) Unless there are compensating intensity and bandwidth changes, a band shift must yield both a negative and a positive intensity difference.

(43) Miskowski, V. M.; Thich, J. A.; Solomon, R.; Schugar, H. J. *J. Am. Chem. Soc.* **1976**, *98*, 8344.

(44) Yandell, J. K., personal communication.

(45) Amundsen, A. R.; Whelan, J.; Bosnich, B. *J. Am. Chem. Soc.* **1977**, *99*, 6730.